Hydrogenation of CO in the Presence of Fe-Containing Materials Based on Carbon Supports

M.I. Ivantsov*, K.O. Krysanova, A.A. Grabchak, M.V. Kulikova

A.V. Topchiev Institute of Petrochemical Synthesis, RAS, 29, Leninsky prospekt, Moscow, Russia

Article info	Abstract
	Hydrothermal carbonization of lignin was used to prepare a precursor of a carbon-containing support to obtain supported iron-containing catalysts for the hydrogenation of carbon monoxide. In the paper, the possibility of forming a carbon support prone to the deposition of metal ions was investigated. Deep structural transformations occurring in the polymer matrix of lignin were demonstrated by FTIR spectroscopy. The thermal stability of the support material was determined by thermal analysis in the region up to 400 °C. The formation of magnetite nanoparticles with a size of about 7–8 nm at the stage of preliminary calcination of the metal-carbon system was shown by X-ray diffraction analysis (XRD). It was found that the resulting systems have high activity comparable to the activity of the system based on activated carbon: the conversion of carbon monoxide reached 98%, the yield of C_{5+} hydrocarbons reached 72 g/m³.

1. Introduction

One of the directions of modern science is the search for new catalytic materials and the improvement of existing ones. This is especially true for technologies associated with the use of carbon oxides, in particular for the Fischer-Tropsch process (hydrogenation of carbon monoxide), which, being the second stage of the XTL processes, allows you to convert various carbon-containing raw materials (biomass – BTL, gas – GTL, coal – CTL) into artificial oil [1, 2], alcohols [3], olefins [4]. The process predominantly implements various reactions associated with the hydrogenation of carbon monoxide, CO transformations [5, 6]:

$$nCO+(2n+1)H_2 \rightarrow C_nH_{2n+2}+nH_2O \qquad (1)$$

$$nCO+2nH_2 \rightarrow C_nH_{2n}+nH_2O \qquad (2)$$

$$nCO+2nH_2 \leftrightarrow C_nH_{2n+1}OH+(n-1)H_2O \qquad (3)$$

$$CO+3H_2 \rightarrow CH_4+H_2O \qquad (4)$$

$$2CO \rightarrow CO_2+C \qquad (5)$$

$$CO+H_2O \leftrightarrow CO_2+H_2 \qquad (6)$$

The Fischer-Tropsch process is catalytic and is catalyzed by VIII group metals [7, 8], but cobalt [9] and iron [10] are widely used.

The properties of catalysts depend on the conditions and methods of synthesis [11, 12], precursors of the active phase [13, 14], and the nature of the support [15], since the interaction between the support and the active phase is possible, which directly affects the catalytic properties of the system [16]. An extensive class of carriers is carbon materials, the distinguishing property of which is the weak interaction between the catalyst particles and the support [17, 18].

Various carbon-containing carriers are being investigated as carriers of the active phase in the hydrogenation of carbon monoxide for the different target products. In [19], on a catalyst representing an iron-containing system supported on activated carbon, the conversion of carbon monoxide reached 74%, and the selectivity for methane did not exceed 2%. On an iron-containing system

*Corresponding author.
E-mail: ivantsov@ips.ac.ru

representing activated carbon treated with $KMnO_4$, olefins were obtained with a selectivity of about 26–40% and a carbon monoxide conversion of 85–97% [20]. The carbon carriers obtained during the synthesis of the catalyst are also studied, in [21] the system obtained by the pyrolysis of Prussian Blue is studied as a catalyst for the production of alcohols from CO and H_2, and 16% CO conversion and 30% selectivity for the formation of alcohols are achieved on it. In [22], an iron-containing material obtained based on metal-organic frameworks (MOFs) is studied, in the presence of the resulting system, the selectivity for C_{5+} hydrocarbons exceeded 85%, and the selectivity for methane formation was 2.44% at a conversion of 9.61%. Systems deposited on nanotubes are also studied, in [23] iron-containing catalysts on N, O – functionalized carbon nanotubes are described, on which the formation of C2-C7 olefins from 72, 4% selectivity at a conversion not exceeding 10%.

It is also worth noting that carbon systems-coals, nanotubes, etc. are hydrophobic materials [24], and for successful sorption of metal ions, additional procedures are required to increase the number of active groups on the support surface [25].

The production of carbon supports can be carried out from carbon-containing raw materials of plant origin, in particular lignin, which today is one of the most common types of waste of organic origin obtained as a result of processing lignocellulosic biomass in the pulp-and-paper industry. According to literature data, its annual growth as a by-product of industrial production is about 150–180 million tons [26]. Despite the fact that lignin is the most common source of stable aromatic compounds in nature, as a rule, it is not subjected to further processing due to its inherent heterogeneity, but is mainly burned as a fuel [27]. The structure of lignin is described in sufficient detail in the literature [28]. It is an amorphous three-dimensional polymer consisting mainly of p-hydroxyphenyl (H), guaiacyl (G) and syringyl (S) units [29], the bond of which is mainly carried out through C-O (for example, β-O-4, α-O-4 and 4-O-5) and C-C (e.g. β-β, β-5 and 5-5) [30].

The possibility of deeper processing of natural polymers, in particular lignin, will make it possible to create a new subclass of catalysts based on carbon-containing supports. However, lignin, like another type of biomass, has some disadvantages that prevent its direct use as a carbon support, namely, the presence of low thermal stability, which, under the conditions of most catalytic processes, will lead to the destruction of the initial biopolymer matrix with the formation of by-products of the reaction.

The use of hydrothermal carbonization (HTC), a process occurring at temperatures of 180–250 °C in a subcritical water environment, for processing lignin will not only increase the thermal stability of the material but also form a carbon matrix capable of sorption of active metal ions. The transformations taking place in the raw material make it possible to perform hydrolysis at ester bonds, and also lead to the elimination of side groups and the formation of a polyconjugated structure [31]. The presence of polyconjugated structures and active oxygen-containing groups on the surface of the carbon material formed in the HTC process makes it possible to use the resulting material for efficient chemisorption of metals active in catalysis [32].

Previously, we have shown the possibility of forming catalytically active systems based on synthetic and natural polymers that form a joint "metal salt-polymer" system by the method of organic matrices [33–36] under conditions of their heat treatment. The physicochemical properties of composite materials obtained by this method depend on a large number of parameters: temperature, exposure time, nature of polymers, etc. The use of the HTC method will make it possible to obtain a carbon material under "softer" temperature conditions of formation, which makes it possible to abandon the high-temperature oxidative stage of the functionalization of the surface of carbon-containing material.

The purpose of this work was to develop a method for obtaining a carbon-containing support from a natural polymer, lignin, subjected to hydrothermal carbonization. Also, the work will implement the synthesis of supported iron-containing catalysts from two types of supports: based on activated carbon and based on hydrothermally carbonized lignin, and determine the patterns of the process of carbon monoxide hydrogenation in the presence of the above catalysts.

2. Experimental

Hydrolytic lignin (TU 64-11-05-87, Industrial Group LLC) was used as a raw material for the production of a lignin-based catalyst.

BAU-A activated carbon (GOST 6217-74, Perm Sorbent Plant UralChemSorb LLC) was used as a raw material for the production of a catalyst on BAU.

Iron nitrate (Fe(NO$_3$)$_3$·9H$_2$O, Extra pure, Scharlau Chemie S.A, Spain) was used as a precursor of iron-containing particles.

Carbon monoxide (CO, Extra pure, LLC "PTC Cryogen", Russia), hydrogen (H2, pure first grade (99.999%) (LLC "NII KM", Russia), nitrogen (N$_2$, Extra pure, LLC "PTC Cryogen", Russia) was used for catalytic tests.

Hydrogen (H2, pure first grade (99.999%), helium (high purity brand 5.0 (99.999%) LLC "NII KM", Russia), synthetic air (zero air) (20.00 vol.% of O$_2$ and 80.00 vol.% of N$_2$, LLC "PTC Cryogen", Russia) was used for analytical investigation.

2.1. Precursor preparation for lignin-based catalyst

Hydrothermal carbonization of lignin was carried out in a 0.5 L autoclave steel reactor equipped with a mechanical stirrer, thermocouple, pressure gauge, tube furnace, and isothermal regulator at a temperature of 230 °C. Raw materials (lignin) with a weight of 30 g were mixed with water in a weight ratio of 1:4 to dry raw materials and placed in a reactor. The reactor was heated to the required temperature and kept in the isothermal mode for 24 h. Then the reactor was cooled to room temperature. The resulting suspension was separated on a filter into a solid residue and a liquid (the pore size of the filter paper was 3–5 μm). Filtration was carried out in a natural way, without additional influences. Drying of the solid residue was carried out at 105 °C for 24 h. Further in the paper, the resulting carbon material is labeled as HTC-Lignin.

2.2. Catalyst synthesis

The catalysts were obtained with use of impregnation by moisture capacity.

To obtain a lignin-based catalyst, the dried solid residue of hydrothermal carbonization weighing 3.54 g was impregnated with 5.11 g of iron nitrate dissolved in 6.4 g of an aqueous-alcoholic solution (1:1 vol.). The resulting mixture was dried in a water bath at a constant temperature of 96 °C. After complete drying, the sample was calcined in a fixed bed reactor in an inert atmosphere at 400 °C for 1 h. Further in the paper, the resulting catalyst is labeled as Fe/HTC-Lignin.

To obtain a catalyst based on BAU, activated carbon weighing 3.51 g was impregnated with 5.06 g of iron nitrate (Fe(NO$_3$)$_3$·9H$_2$O dissolved in 4.74 g of an aqueous-alcoholic solution (1:1 vol.). The resulting mixture was dried in a water bath at a constant temperature of 96 °C. After complete drying, the sample was calcined in a fixed bed reactor in an inert atmosphere at 400°C for 1 h. Further, in the paper, the resulting catalyst is labeled as Fe/BAU.

2.3. Catalytic tests

Hydrogenation of carbon monoxide was carried out in a flow catalytic system with fixed bed reactor. To reduce the resistance of the catalyst bed to the gas flow and prevent sintering, the catalyst was diluted with quartz in a volume ratio of 5:3, respectively. The synthesis was carried out in a continuous mode at a pressure of 20 bar and a space velocity of the initial synthesis gas of 1000 h^{-1} (molar ratio CO:H$_2$ = 1:1, as an internal standard used 5 vol.% N2) in the temperature range from 260 °C to 340 °C. The temperature was raised stepwise (by 20 °C every 12 h). At the end of each isothermal mode, gas and liquid products were sampled. Before catalytic tests, the samples were preliminarily activated with carbon monoxide at a temperature of 400 °C, a pressure of 20 bar, and CO space velocity of 1000 h^{-1}.

2.4. Analysis of reagents and reaction products

The initial synthesis gas and gaseous synthesis products were analyzed on a Kristalluks-4000 M chromatograph (Russia) with two chromatographic columns. Helium was used as a carrier gas, and a katharometer was used as a detector. To separate gas mixtures, a column filled with CaA molecular sieve (3 mm × 3 m) and a HayeSep R column (3 m × 3 mm) were used. The analysis was carried out in the following mode: isothermal 50 °C, 5 min, 50–200 °C thermally programmed mode – 8 °C min^{-1}.

Liquid hydrocarbons were analyzed by gas-liquid chromatography (GLC) on a Kristalluks-4000 M chromatograph (Russia), a detector was a flame ionization one, and a carrier gas was helium. A 50 m × 0.32 mm capillary column filled with OV-351 was used to separate the mixture of hydrocarbons. Temperature-program mode: 50 °C (2 min); 50–260 °C, 6 °C/min; 260–270 °C, 5 °C/min; 270 °C (10 min).

The activity of the catalyst was evaluated by the following indicators: CO conversion (K$_{CO}$, %) – CO (percentage of the weight of reacted carbon monoxide to the weight of CO supplied to the reaction zone):

$$K_{CO} = \frac{m_{co}^{in} - m_{Co}^{out}}{m_{CO}^{in}} \times 100\% \qquad (7)$$

Product yield (number of grams of product obtained by passing 1 m³ of synthesis gas through the catalyst):

$$Y_{Product} = \frac{m_{product}}{V_{syn-gas}} \qquad (8)$$

2.5. Physical and chemical studies

2.5.1. X-ray diffraction (XRD)

X-ray phase analysis (XRPA) was performed on a Rotaflex-Ru200-D/max-RC diffractometer (Japan) using CuKα (wavelength 0.154 nm) radiation. The studies were carried out at the following acquisition parameters – 100 mA and 50 kV. The average size of coherent scattering regions (CSR) was calculated by the Debye-Scherrer method.

2.5.2. FT-IR spectroscopy

IR spectra were recorded by reflection on a Hyperion-2000 IR microscope coupled to an IFS-66 v/s Bruker IR spectrometer (range 600–4000 cm⁻¹) (Germany).

2.5.3. Thermograviometric studies

The thermal behavior of precursors of catalytic systems (weight change and thermal effects) during temperature-programmed heating was studied on a TGA/DSC 3+ Mettler Toledo instrument (Switzerland). The measurements were carried out in corundum crucibles with a volume of 150 μl in the temperature range from room temperature to 900 °C at a heating rate of 10 deg/min. The flow rate of the inert gas (argon) was 70 ml/min.

2.5.4. Morphological studies

Surface characteristics – specific surface area and average pore size – were measured at Micromeritics ASAP 2020 (USA) by measuring N2 adsorption-desorption isotherms at –196 °C. The specific surface was obtained using the BET model. The average pore size was calculated by the BJH method.

2.5.5. Microscopic measurements

The target-oriented approach was utilized for the optimization of the analytic measurements [37].

Before measurements, the samples were mounted on a 3 mm copper grid with carbon film and fixed in a grid holder. Samples morphology was studied using Hitachi transmission electron microscope (TEM). Images were acquired in bright-field TEM mode at 100 kV accelerating voltage.

3. Results and discussion

In the course of the work, two carbon-containing catalysts for the CO hydrogenation process were studied: a catalyst based on hydrothermally carbonized natural raw materials (lignin) and a catalyst based on a traditional carbon sorbent (activated carbon of the BAU brand).

The resulting systems were studied by various physicochemical methods to determine the ongoing changes in the structure of the formed materials. In order to establish structural changes that occur during the formation of carbon support and a catalyst based on it, the following objects were studied: initial lignin, hydrothermally treated lignin (HTC-Lignin) and iron-supported catalyst (Fe/HTC-Lignin) (Fig. 1).

According to the data of FT-IR spectroscopy, it was found that in the process of hydrothermal carbonization, the splitting of ether bonds in aryl ethers occurs (the absorption band of C-O in aryl-O-CH₃ and aryl-OH is 1032 cm⁻¹) and alkyl ethers, however, at In this case, there is no significant decrease in the splitting of C-O-C bonds (absorption band is 1056 cm⁻¹) from the aryl-O bond in aryl-OH and aryl-O-CH₃ (absorption band is 1212 cm⁻¹) [38], which may indicate the preservation of the aromatic structures of the original lignin.
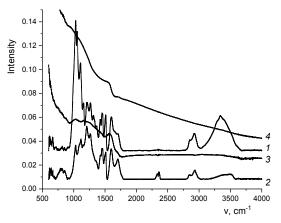

Fig. 1. IR-Fourier spectroscopy of samples: (1) – initial lignin; (2) – lignin obtained by hydrothermal treatment at 230 °C (HTC-Lignin); (3) – catalyst obtained by impregnation and heat treatment of lignin (Fe/HTC-Lignin); (4) – catalyst obtained by impregnation and heat treatment of activated carbon (Fe/ BAU).

Also, in the process of hydrothermal carbonization, the structure of lignin is destroyed with the formation of C-O fragments of the guaiacyl ring (absorption band is 1268 cm^{-1}). The decrease in intensity from the band of in-plane deformation vibrations of phenolic O-H groups (absorption band at 1366 cm^{-1}) and stretching vibrations of phenolic O-H groups (absorption band at 3450 cm^{-1}) may indicate the ongoing process of cross-linking of fragments of the lignin structure. The intensity from skeletal vibrations of the aromatic ring (absorption band at 1424, 1452, 1511, 1600 cm^{-1}) does not change after the hydrothermal treatment of lignin, which indicates the preservation of aromatic fragments of the structure of the original lignin. An increase in intensity from the absorption band at 1711 cm^{-1} in the HTC-Lignin sample, corresponding to stretching vibrations of the C=O bond in nonconjugated ketones, carbonyl, carboxyl, and ether groups, as well as an increase in the intensity of the band at 814 cm^{-1} (out-of-plane deformation vibrations of the C-H bond in the aromatic ring), demonstrate the occurrence of oxidative processes in hydrocarbon chains. The absorption bands in the region of 2340–2360 cm^{-1} found in the spectrum of the HTC-Lignin sample are characteristic of sorbed CO_2 molecules, which are formed during the complete oxidation of the lignin functional groups and are retained in the structure of the carbon support. Separately, it is worth noting the decrease in the intensity of a wide absorption band in the region of 3030–3600 cm^{-1}, related to the vibration of the O-H group, which indicates the ongoing processes of lignin dehydration in the HTC process.

The data of FT-IR spectroscopy testify to the structural changes of the HTC-Lignin sample, associated with a decrease in the number and oxidation of the functional groups of aromatic rings, as well as with the ongoing process of dehydration of the material and cross-linking of fragments of its structure. It should be noted that the hydrothermal treatment of lignin did not affect the integrity of the aromatic rings.

The presence of oxygen-containing groups in the composition of the Fe/HTC-Lignin material (Fig. 1) may indicate the formation of a functionalized carbon surface with anchor groups during the synthesis of the material, and not during an additional stage of processing. It is possible to immobilize iron ions on the support surface, which, with further additional heat treatment at 400 °C, contributes to the formation of a catalytic system of the metal-containing support particle type. So, in the composition of the carbon-containing framework of the material HTC-Lignin, oxygen-containing functional groups can be identified by the presence of an absorption band at 1030 cm^{-1}, corresponding to the C-O group in aryl-O-CH$_3$ and aryl-OH, and absorption band at 1699 cm^{-1}, related to the bond in non-conjugated ketones, carbonyl, carboxyl and ether groups. Absorption bands related to vibrations of aromatic ring groups are widely represented: in-plane deformation vibrations of aromatic C-H bonds (1161 cm^{-1}), vibrations of the guaiacyl ring with stretching vibrations of C-O groups (1256 cm^{-1}), skeletal vibrations of the aromatic ring (absorption bands at 1428 and 1576 cm^{-1}).

For comparison with the Fe/HTC-Lignin sample (Fig. 1), the absorption spectrum of the Fe/BAU sample is added. The spectrum of the Fe/BAU sample (Fig. 1) is an IR spectrum of typical carbon material, in which there are no bands and an increase in the general absorption background in the long-wavelength region of the spectrum, which is a direct indication of the high content of oxidized forms in this carbon material and the possible presence of iron oxides (Fe-O absorption band, 567 cm^{-1} [39] in Fe_3O_4 and 560 cm^{-1} in Fe_2O_3 [40].

When comparing the spectra of the two catalysts, it can be concluded that broad overlapping absorption bands from the original lignin structure remain in the Fe/HTC-Lignin sample, while individual bands and, as a result, groups cannot be distinguished on the Fe/BAU surface. Special attention should be paid to the absorption band at 1699 cm^{-1}, which is present both in Fe/BAU and in Fe/HTC-Lignin, which indicates the presence of oxidized oxygen groups.

One of the important characteristics of activated carbons is their high specific surface area, which makes morphological studies extremely relevant (Table 1). During hydrothermal carbonization, a carbon structure is formed based on lignin chains. A material is formed with a small specific surface area (by 23 times) compared to the material on activated carbon and a large pore size (by 2 times) relative to activated carbon. The obtained values of surface characteristics correlate with the data obtained on a sample of biochar synthesized from lignin at 150°C in [41] and the specific surface area is 2.53 m^2/g, and the pore size is 17.1 Å.

The phase composition of the objects used in the work was studied by X-ray phase analysis. The X-ray pattern of the initial lignin, the HTC-Lignin sample, and the Fe/HTC-Lignin catalyst is shown in Fig. 2.

Table 1
Specific surface area and average pore size
of catalytic systems

Sample	S_{sp}, m²/g	d_{pore}, Å
Fe/HTC-Lignin	21	74
Fe/BAU	493	37

The initial lignin, like the sample HTC-Lignin, is an X-ray amorphous material. A wide halo in the region of 20–30° indicates a slight ordering of the biopolymer fragments [42]. Slight peaks observed on the X-ray pattern indicate the presence of quartz, which was originally present in the raw material (lignin). The Fe_3O_4 reflections (2θ of 30.08; 35.43; 43.05; 56.94; 62.52° (JCPDS-79-0419)) are fixed on the X-ray pattern of the Fe/HTC-Lignin sample, which may indicate the interaction of iron (III) ions in the Fe/HTC-Lignin sample and the flow of the process of reduction of Fe(III) to Fe(II) during thermal treatment of the catalyst precursor. The phase composition of the reference sample was also studied by X-ray phase analysis (see Fig. 2). The Fe/BAU diffraction pattern also shows reflections of magnetite Fe_3O_4 (2θ of 30.08; 35.43; 43.05; 56.94; 62.52° (JCPDS-79-0419)). The fact of magnetite formation when using carbon supports was also reported in [43].

Using the Debye-Scherrer method, it was found that the size of crystallites in the Fe/HTC-Lignin sample is about 7–8 nm, while the estimate of the crystallite size in the Fe/BAU sample showed that their size was 2–3 nm.

(a)

(b)

Fig. 3. Microphotograph of samples of iron-containing catalysts: (a) – Fe/BAU; (b) – Fe/HTC-Lignin.

Microscopic studies of catalytic systems make it possible to estimate the size of nanoparticles of the iron-containing phase distributed in a carbon-containing matrix (Fig. 3). The results of microscopy are consistent with the results of the assessment of the size of crystallites: the micrograph of the Fe/BAU sample shows the formation of particles with a size of 1–3 nm, while the Fe/HTC-Lignin sample shows particles with a size of 3–15 nm.

The thermal stability of the samples was evaluated by thermogravimetric (Fig. 4). The weight loss for the HTC-Lignin sample at 400 °C was 14%, while the weight loss for the initial lignin was
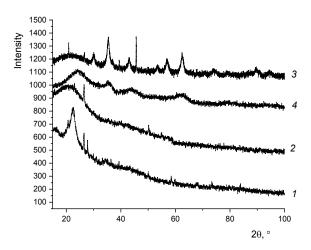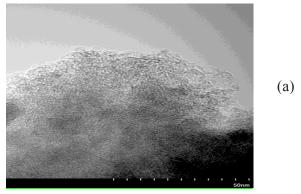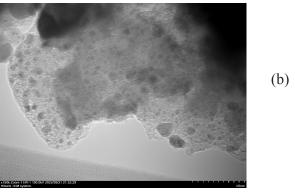
Fig. 2. X-ray patterns of samples: (1) – original lignin; (2) – lignin subjected to hydrothermal treatment at 230 °C (HTC-Lignin); (3) – catalyst obtained by impregnation and heat treatment of lignin (Fe/HTC-Lignin); (4) – catalyst obtained by impregnation and heat treatment of activated carbon (Fe/BAU).
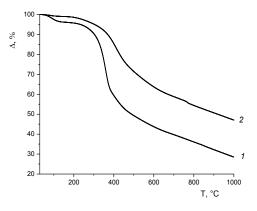
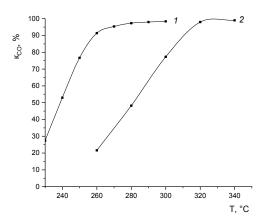Fig. 4. Thermogravigram of the initial lignin sample (1) and HTC-Lignin sample (2).

Fig. 5. Dependence of the carbon monoxide conversion index on the experimental temperature for Fe/BAU (1) and Fe/HTC-Lignin (2) samples.

much higher (40%), which indicates that a more thermally stable carbon matrix is formed during hydrothermal carbonization, which makes it possible to use it as a support of catalysts for a wide range of processes, and in particular for the process of hydrogenation of carbon monoxide.
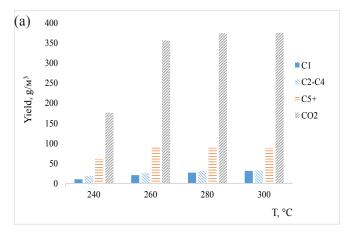
The resulting systems were studied under the conditions of hydrogenation of carbon monoxide (Fig. 5). The systems showed high activity in CO hydrogenation (see Fig. 5), and they achieved almost 100% conversion of carbon monoxide.

For Fe/BAU, the optimum synthesis temperature at which 100% CO conversion was achieved was 260 °C. The highest catalytic activity of the Fe/HTC-Lignin system was observed at higher temperatures compared to Fe/BAU (T_{opt} = 320 °C).

The formation of C_{5+} hydrocarbons occurs more intensively in the Fe/BAU system (Fig. 6a): the C_{5+} yield was 23% higher than in the case of the Fe/HTC-Lignin system (Fig. 6b). Based on the data (see Fig. 6b), it can be assumed that the intensification of the formation of methane, C_2-C_4 hydrocarbons and CO_2 when using the Fe/HTC-Lignin system was associated with a higher operating temperature of the lignin-based system. A high release of CO_2 is also observed in activated carbon systems described in [44], the formation of CO_2 accounts for about 38–40%, it can also be noted that in this system the formation hydrocarbons C_2-C_4 and hydrocarbons C_{5+} occurs with approximately the same proportion – 42–46% (excluding CO_2), while in our case there is a shift towards the formation of longer-chain molecules. Comparable data are given in the review [45] since C_{5+} hydrocarbons are predominantly formed on an iron-containing system on activated carbon without taking into account the formation of carbon dioxide.

The group and fractional compositions of hydrocarbons (Table 2) indicate that the substrate on the Fe/HTC-Lignin catalyst is more prone to polymerization than on Fe/BAU, which may be due to the larger particle size of the system [46] obtained based on lignin. This may also be due to the large pore size of the lignin based carbon matrix [47]. Separately, it is worth paying attention to the significant yield of CO_2, both on Fe/BAU and on Fe/HTC-Lignin, which can be explained by the small particle size and the presence of the Fe_3O_4 phase in the sample, on which the water shear reaction is accelerated [48].

A significant difference is observed in the group composition. On the Fe/BAU sample, n-alkanes are predominantly formed, while in the target product on the Fe/HTC-Lignin sample, the content of iso-paraffins is high, which, unlike normal paraffins, are characterized by high antiknock characteristics and a lower pour point. Separately, it is worth noting the higher content of olefins in the synthesis products on the Fe/BAU catalyst in comparison with Fe/HTC-Lignin.
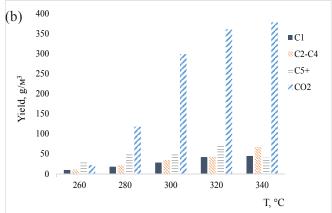

Fig. 6. The main indicators of the hydrogenation of carbon monoxide (II) in the presence of deposited metal-carbon-containing systems: (a) – Fe/BAU; (b) – Fe/HTC-Lignin.

Table 2

Fractional and group composition of the resulting hydrocarbons

Sample	n-paraffin	Isoparaffin	Olefins	C_5-C_{10}	C_{11}-C_{18}	C_{19+}	α
Fe/BAU	41.5	30.2	28.2	69.8	25.1	5.0	0.75
Fe/HTC-Lignin	34.1	48.2	16.4	56.1	33.1	9.5	0.76

It should also be emphasized that the polymerization activity is higher on the Fe/HTC-Lignin sample (chain growth index (α) = 0.79) than on the Fe/BAU sample, which may indicate the formation of various active centers depending on the nature of the carbon support. This effect can be associated with the physicochemical properties of the formed nanoparticles of the iron-containing phase, as well as with the influence of the carbon-containing matrix.

Conclusion

In this work, we screened the catalytic properties of catalysts based on carbon supports in the carbon monoxide hydrogenation reaction. We showed the fundamental possibility of synthesizing catalytic systems from carbon material obtained by hydrothermal carbonization of lignin, one of the main biopolymers on the planet. The synthesized catalytic systems showed high catalytic activity. The group composition of liquid hydrocarbons is dominated by iso-paraffins, and the fractional composition is dominated by the gasoline fraction. The resulting material is promising as catalyst support; however, to increase the polymerization activity of the centers of the catalytic system, there is a need to introduce additional promoting additives. The performed procedure for the hydrothermal treatment of lignin made it possible, under "mild" conditions for the implementation of the process (temperature not higher than 230 °C, absence of an activation stage) to form a system with polyconjugated regions in the polymer chain and heteroatoms that can be used as "anchors" for the immobilization of the metal-containing phase.

Acknowledgements

References

[1]. J. van de Loosdrecht, F.G. Botes, I.M. Ciobica, A.C. Ferreira, et al., Comprehensive Inorganic Chemistry II (Second Edition) 7 (2013) 525–557. DOI: 10.1016/B978-0-08-097774-4.00729-4

[2]. M. Martinelli, M.K. Gnanamani, S. LeViness, G. Jacobs, et al., *Appl. Catal. A* 608 (2020) 117740. DOI: 10.1016/j.apcata.2020.117740

[3]. Y.-P. Pei, J.-X. Liu, Y.-H. Zhao, Y.-J. Ding, et al. *ACS Catal.* 5 (2015) 3620–3624. DOI: 10.1021/acscatal.5b00791

[4]. Z. Gholami, F. Gholami, Z. Tišler, J. Hubáček, et al., *Catalysts* 12 (2022) 174. DOI: 10.3390/catal12020174

[5]. Gerard P. van Der Laan, A.A.C.M. Beenackers, *Cat. Rev.* 41 (1999) 255–318. DOI: 10.1081/CR-100101170

[6]. Olusola O. James, Biswajit Chowdhury, M. Adediran Mesubic, Sudip Maity, *RSC Adv.* 2 (2012) 7347–7366. DOI: 10.1039/C2RA20519J

[7]. Z. Teimouri, N. Abatzoglou, A.K. Dalai, *Catalysts* 11 (2021) 330. DOI: 10.3390/catal11030330

[8]. H. Jahangiri, J. Bennett, P. Mahjoubi, K. Wilson, et al., *Catal. Sci. Technol.* 4 (2014) 2210. DOI: 10.1039/c4cy00327f

[9]. Z. Gholami, Z. Tišler, V. Rubáš, *Cat. Rev.* 63 (2021) 512–595. DOI: 10.1080/01614940.2020.1762367

[10]. E. de Smit, B.M. Weckhuysen, *Chem. Soc. Rev.* 37 (2008) 2758–2781. DOI: 10.1039/B805427D.

[11]. Y. Yang, H. Zhang, H. Ma, W. Qian, et al., *Top Catal.* (2022). DOI: 10.1007/s11244-022-01684-5

[12]. S.A. Gardezi, J.T. Wolan, B. Joseph, *Appl. Catal. A* 447–448 (2012) 151–163. DOI: 10.1016/j.apcata.2012.09.035

[13]. L. Fratalocchi, C.G. Visconti, L. Lietti, *Appl. Catal. A* 595 (2020) 117514. DOI: 10.1016/j.apcata.2020.117514

[14]. J.L. Eslava, A. Iglesias-Juez, M. Fernández-

García, A. Guerrero-Ruiz, et al., *Appl. Surf. Sci.* 447 (2018) 307–314. DOI: 10.1016/j.apsusc.2018.03.207.

[15]. Y. Han, G. Xiao, M. Chen, S. Chen, et al., *Catal. Today* 375 (2021) 1–9. DOI: 10.1016/j.cattod.2020.04.035

[16]. H. Wan, B. Wu, H. Xiang, Y. Li, *ACS Catal.* 2 (2012) 1877–1883. DOI: 10.1021/cs200584s

[17]. A. Wang, M. Luo, B. Lü, Y. Song, et al., *Mol. Catal.* 509 (2021) 111601. DOI: 10.1016/j.mcat.2021.111601

[18]. Y. Chen, J. Wei, M.S. Duyar, V.V. Ordomsky, et al., *Chem. Soc. Rev.* 50 (2021) 2337–2366. DOI: 10.1039/D0CS00905A

[19]. H.Y. Ban, Z.W. Wang, Z.Q. Wang, Z.G. Fang, *Adv. Mater. Res.* 805-806 (2013) 232–235. DOI: 10.4028/www.scientific.net/amr.805-806.232

[20]. Z. Tian, C. Wang, Z. Si, L. Ma, et al., *Appl. Catal. A* 541 (2017) 50–59. DOI: 10.1016/j.apcata.2017.05.001

[21]. Y. Chen, L. Ma, R. Zhang, R. Ye, et al., *Appl. Catal. B* 312 (2022) 121393. DOI: 10.1016/j.apcatb.2022.121393

[22]. M.U. Nisa, Y. Chen, X. Li, X. Jiang, et al., *J. Taiwan Inst. Chem. Eng.* 131 (2022) 104170. DOI: 10.1016/j.jtice.2021.104170

[23]. Z. Zhang, J. Zhang, X. Wang, R. Si, et al., *J. Catal.* 365 (2018) 71–85. DOI: 10.1016/j.jcat.2018.05.021

[24]. M.M. Abu-Omar, K. Barta, G.T. Beckham, J.S. Luterbacher, et. al., *Energy Environ. Sci.* 14 (2021) 262–292. DOI: 10.1039/D0EE02870C

[25]. Y. Cao, M. He, S. Dutta, G. Luo, et al., *Renew. Sustain. Energy Rev.* 152 (2021) 111722. DOI: 10.1016/j.rser.2021.111722

[26]. M.V. Chudakova, M.V. Kulikova, M.I. Ivantsov, G.N. Bondarenko, et al., *Pet. Chem.* 57 (2017) 694–699. DOI: 10.1134/S0965544117080023

[27]. R.A.C. Gomide, A.C.S. de Oliveira, D.A.C. Rodrigues, C.R. de Oliveira, et al., *J. Polym. Environ.* 28 (2020) 1326–1334. DOI: 10.1007/s10924-020-01685-z

[28]. J. Hu, Q. Zhang, D.J. Lee, *Bioresour. Technol.* 247 (2018) 1181–1183. DOI: 10.1016/j.biortech.2017.08.169

[29]. U. Kamran, Y.-J. Heo, J.W. Lee, S.-J. Park, *Micromachines* 10 (2019) 234. DOI: 10.3390/mi10040234

[30]. S.N. Khadzhiev, M.V. Kulikova, M.I. Ivantsov, L.M. Zemtsov, et al., *Pet. Chem.* 56 (2016) 522–528. DOI: 10.1134/S0965544116060049

[31]. M.V. Kulikova, M.V. Chudakova, M.I. Ivantsov, A.E. Kuz'min, et al., *J. Braz. Chem. Soc.* 32 (2021) 287–298. DOI: 10.21577/0103-5053.20200179

[32]. Q. Yan, J. Street, F. Yu, *Biomass Bioenerg.* 83 (2015) 85–95. DOI: 10.1016/j.biombioe.2015.09.002

[33]. J.A. Libra, K.S. Ro, C. Kammann, A. Funke, et al., *Biofuels* 2 (2011) 71–106. DOI: 10.4155/bfs.10.81

[34]. X. Liu, F.P. Bouxin, J. Fan, V.L. Budarin, et al., *J. Hazard Mater.* 402 (2021) 123490. DOI: 10.1016/j.jhazmat.2020.123490

[35]. G.R. McMeeking, N. Good, M. Petters, G. McFiggans, et al., *Chem. Phys.* 11 (2011) 5099–5112. DOI: 10.5194/acpd-11-917-2011

[36]. A. Mirzaei, K. Janghorban, B. Hashemi, S.R. Hosseini, et al., *Process. Appl. Ceram.* 10 (2016) 209–217. DOI: 10.2298/PAC1604209M

[37]. V.V. Kachala, L.L Khemchyan, A.S. Kashin, N.V. Orlov, et al., *Russ. Chem. Rev.* 82 (2013) 648–685. DOI: 10.1070/RC2013v082n07ABEH004413

[38]. A.N. Pour, M.R. Housaindokht, *J. Ind. Eng. Chem.* 20 (2014) 591–596. DOI: 10.1016/j.jiec.2013.05.019

[39]. A.H. Rezayan, M. Mousavi, S. Kheirjou, G. Amoabediny, et al., *J. Magn. Magn. Mater.* 420 (2016) 210–217. DOI: 10.1016/j.jmmm.2016.07.003

[40]. G. Speranza, *C* 5 (2019) 84. DOI: 10.3390/c5040084

[41]. Y. Tian, Y. Yin, H. Liu, H. Zhou, *J. Water Process Eng.* 46 (2022) 102583. DOI: 10.1016/j.jwpe.2022.102583

[42]. Y. Wang, W. Ma, Y. Lu, J. Yang, et al., *Fuel* 82 (2003) 195–213. DOI: 10.1016/S0016-2361(02)00154-0

[43]. S.S. Wong, R. Shu, J. Zhang, H. Liu, et al., *Chem. Soc. Rev.* 49 (2020) 5510–5560. DOI: 10.1039/D0CS00134A

[44]. W. Ma, Y. Ding, J. Yang, X. Li, et al., *React. Kinet. Catal. Lett.* 84 (2005) 11–19. DOI: 10.1007/s11144-005-0185-6

[45]. M.J. Valero-Romero, M.Á. Rodríguez-Cano, J. Palomo, J. Rodríguez-Mirasol, et al., F*ront. Mater., Sec. Carbon-Based Materials* 7 (2021) 617432. DOI: 10.3389/fmats.2020.617432

[46]. V.O. Kazak, P.A. Chernavskii, G.V. Pankina, A.Y. Khodakov, et al., *Russ. J. Phys. Chem.* 89 (2015) 2032–2035. DOI: 10.1134/S0036024415110060

[47]. A.Y. Khodakov, A. Griboval-Constant, R. Bechara, V.L. Zholobenko, *J. Catal.* 206 (2002) 230–241. DOI: 10.1006/jcat.2001.3496

[48]. A.P. Karmanov, O.Yu. Derkacheva, *Khimija Rastitel'nogo Syr'ja* 1 (2012) 61–70. (in Russian)